EVIDENCE FOR THE PRODUCTION OF *d-d* FUSION NEUTRONS DURING ELECTROLYTIC INFUSION OF DEUTERONS INTO A PALLADIUM CYLINDER

COLD FUSION

TECHNICAL NOTE

KEYWORDS: *D-D fusion neutrons, neutron spectroscopy, palladium*

MICHAEL BITTNER, G. LUDWIG, ANDREAS MEISTER, J. MÜLLER, DETLEF OHMS, ELIEF PAFFRATH, DIETMAR RAHNER, RAINER SCHWIERZ, DIETER SEELIGER, P. STIEHL, KLAUS WIESENER, and PETER WÜSTNER

Dresden University of Technology, Physics and Chemistry Departments
Mommsenstrasse 13, O-8027 Dresden, Federal Republic of Germany

Received August 30, 1990
Accepted for Publication January ? 1991

A lengthy experiment for the observation of deuteron-deuteron (d-d) fusion neutrons emanating from a massive palladium cylinder is described. The experimental results are discussed in the framework of a plasmalike model for fusion in condensed matter, resulting in fusion rates of $\lambda_{d\text{-}d}^{Pl} = (1.19 \pm 0.15) \times 10^{-44}\ s^{-1}$.

INTRODUCTION

Recently, evidence was found in several experiments of weak neutron production by possible deuteron-deuteron (*d-d*) fusion processes in condensed matter.[1-4] After the experiments were confirmed, systematic studies were started.

The experimental method used, which differs from approaches chosen by other groups, was described in Ref. 5. Ir that technical note, the results of investigations that used ordinary water (H_2O) instead of heavy water (D_2O), as well as measurements without electrolytic current, were presented.

For physical discussions, a simple plasma model describing the time structure of possible *d-d* fusion processes is proposed in Ref. 6.

Those two technical notes provide all the details of the experimental methods, data analyses, and arguments concerning the application of the physical model used here. Therefore, the description of the experimental methods and the physical model (including its parameters) is very brief in this technical note. The investigation of long-term effects in the massive Z1 palladium cylinder is described here. This electrode was observed in an experimental cycle at the same time as two other electrodes. Results for those two electrodes (which show similar effects) will be published separately.

EXPERIMENT

The experimental cycle "series 3" described here lasted a total of 786 h, but cylinder Z1 was in the experiment for only 606 h, from the beginning of the cycle. The complete series 3 cycle ran from June 3 to July 7, 1989.

As described in Ref. 5, all measurements were carried out relative to the two other electrodes (cells) in front of the proton-recoil spectrometer (PRS) for fast neutrons but also relative to the empty position (background) in a sequence of 1-h-long measurements. Therefore, each cell was observed near the PRS for part of the cycle. For Z1, a total of 110 measurements was carried out, and during this period, the background was measured 116 times.

The high-purity Z1 palladium cylinder was 23.1 mm in diameter and 19.3 mm long, and it weighed 93.539 g when empty. A platinum grid placed at a distance of ~5 mm around the cylindric surface of the cathode was used as the anode. The electrolysis was performed using a 3 *M* solution of LiOD in redistilled D_2O (99.8% isotope enrichment) with a constant electric current of $I = 4$ A without any interruptions. Periodically, the voltage and the temperature of the cell were recorded. The level of electrolyte in the cell was controlled by feeding it with 0.05 *M* electrolyte or pure D_2O without interrupting the electrolyte current during the time intervals between the hourly measurements.

The stability of the detector and the energy calibration were periodically checked after ~8 h through radioactive sources. The pulse-height spectrum [proton-recoil energy (PRE)] was recorded in 512 channels of a multichannel analyzer as well as in more sensitive broad-channel groups:

1. channel range 2: PRE 1.4 to 2.9 MeV
2. channel range 3: PRE 1.9 to 2.9 MeV
3. channel range 4: PRE 2.9 to 4.1 MeV.

As shown in Ref. 5, the method used has not only the advantage of high sensitivity but also fewer effects on the results of analyses from possible slow drifts. Additionally, for some hypothetical effects caused by cosmic rays, upper limits can be stated. However, the method does not allow the observation of short bursts because all effects are averaged over at least 1 h.

After finishing the experimental cycle, the deuterium content in cell Z1 was determined by weighing. During this cycle,

the electrode was loaded with 1.419 g deuterium, corresponding to a D/Pd atomic ratio of 0.801. This number was obtained by comparing the weight of the dry charged cathode immediately after the end of the experimental cycle with the weights of the pure metallic sample both before charging and after its outgassing at high temperature in a vacuum chamber.

RESULTS

Figure 1 gives the experimental count rates for channel range 3, the most sensitive channel, both with cell Z1 in front of the detector and for the empty position. The integration time for all single measurements is 1 h. Effect and background measurements are distributed almost uniformly, thus avoiding systematic errors from slow background drifts. From this figure, it is clear that to search for such small effects, it is absolutely necessary to measure effect and background simultaneously. This is because the background level cannot be considered completely constant (because, e.g., of variations in cosmic background or slow changes in the neutron-gamma discrimination).

However, even in this presentation, it is evident that up to ~200 h, the effect and background measurements are almost at the same level, whereas the asterisks, on average, might be slightly above the triangles between 300 and 500 h, but this is difficult to recognize visually.

Only very few effect data points are clearly above the background level. This observation is demonstrated quantitatively by the difference in count rates per hour obtained for various broader time intervals, as shown in Table I. For the 0- to 220-h time interval, the difference is even slightly negative. This is the result of the partial absorption of background neutrons by the cell in front of the detector (shadow effect), which is discussed in more detail in Ref. 5. If the effective background reduction by $(-1.4 \pm 1.0)\ h^{-1}$ obtained from measurements without electrolysis current[5] is taken into account, the corrected effect differences indicated in the table are obtained. From this table it may be seen that within the first 200 h of electrolysis, the resulting effect remains zero

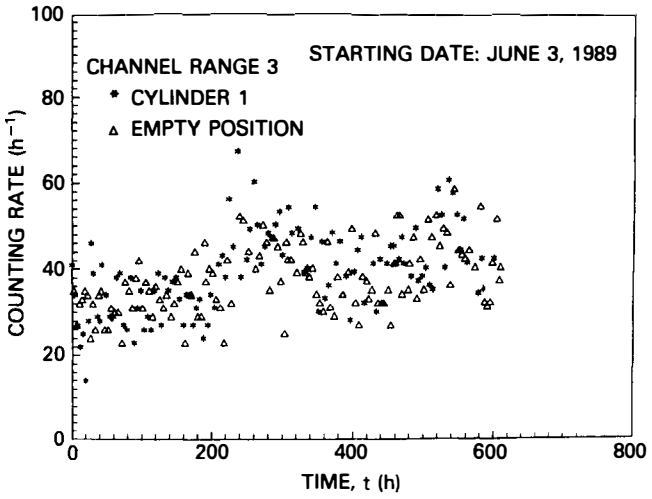

Fig. 1. Experimental count rates in 1-h intervals for cell with Z1 in front of the detector (asterisks) and for the empty position (triangles).

TABLE I

Averaged Effect Minus Background Count Rate Differences*

Time Interval (h)	Measured Difference (h^{-1})	Corrected Difference (h^{-1})
0 to 220	-0.7 ± 0.9	0.7 ± 1.3
240 to 380	$+4.8 \pm 1.3$	6.2 ± 1.6
285 to 315	$+8.1 \pm 1.9$	9.5 ± 2.1
380 to 606	$+2.4 \pm 1.9$	3.8 ± 2.1
0 to 606	$+2.1 \pm 0.9$	3.5 ± 1.3

*For channel range 3 within different time intervals.

to within 1σ. It later increases, giving, on average, a positive effect of $\sim 3\sigma$, and between 285 to 315 h, it even exceeds 4σ. The highest single measurement shows an effect count rate of $(30 \pm 10)\ h^{-1}$.

There are definite positive effects in partial time intervals of a few days' duration in which the background level is almost constant, and there are no intervals showing a similar "negative effect" other than those caused by the shadow effect. Furthermore, the results of simultaneous measurements in the same experimental cycle with the massive slab AH1 were presented in Fig. 18 of Ref. 5 using the same background measurements as are shown in Fig. 1. Within a 280-h interval in that case, a count rate difference of $(-1.3 \pm 1.4)\ h^{-1}$ was observed. From that measurement, upper limits on both the *d-d* reaction effect and the influence of cosmic radiation (including muons) on a fully loaded massive (170-g) palladium sample were derived. During that time, the Z1 cell still showed a definite positive effect. On the other hand, for the 0- to 200-h time interval, where cell Z1 does not show any systematic positive effect, slab AH1 was already active. Moreover, the time intervals of highest activity for Z1 do not coincide with those for AH1. This behavior excludes any external sources of radiation as the origin of the positive effects in cell Z1. The effect level, however, is not constant but fluctuates strongly.

The uncorrected and corrected count rate differences for the 280- to 320-h time interval in channel group 4 amount to $(-0.8 \pm 2.6)\ h^{-1}$ and $(-0.1 \pm 2.6)\ h^{-1}$, respectively. (The shadow effect in channel group 4 is smaller because of the shape of the background neutron spectrum.) It can be concluded that, as expected, there is no effect within this PRE range.

The distributions of background (empty position) and uncorrected count rates relative to a fitted χ^2 minimum background line are shown in Fig. 2. The deviation of the average count rate from zero reflects the uncorrected rates given in Table I. The shape of background count rates within the statistics is reasonably presented by Poisson statistics. Clearly positive effects are observed for the 240- to 380-h time interval. Taking into account the shadow effect would further enhance the magnitude of the positive effects. If the different count rates are averaged over longer time intervals, a pronounced time structure of long-term effects becomes visible. Figure 3 shows count rate differences averaged over 10 and 60 h. The reduced background line due to the shadow effect is also indicated. After averaging fluctuations and brief peaks

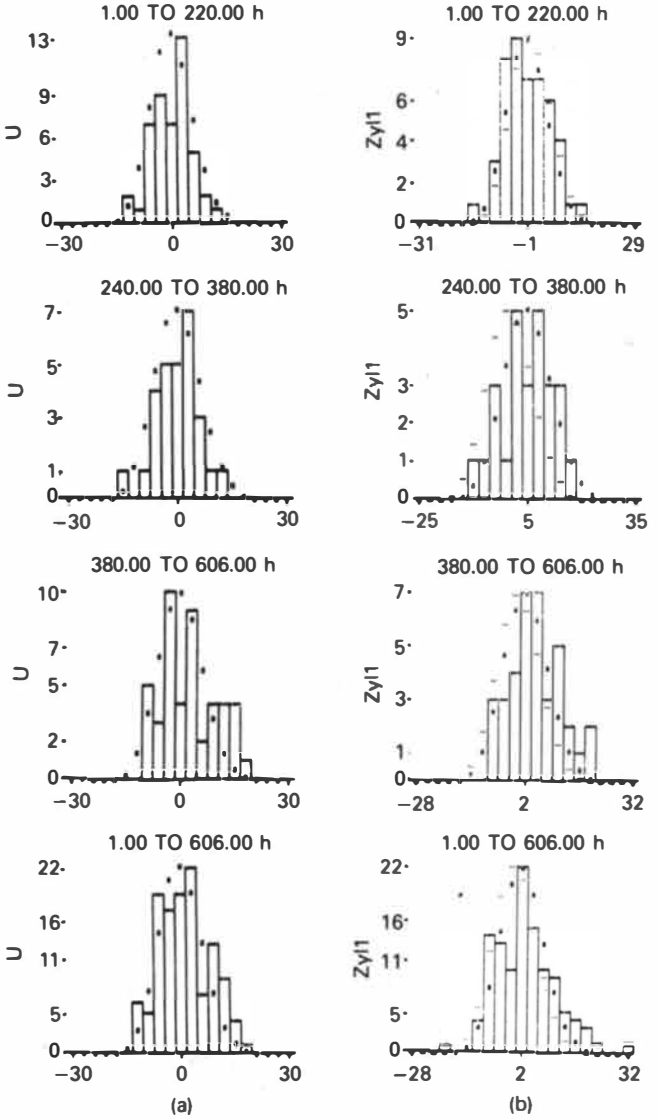

Fig. 2. Distributions of count rate differences for (a) empty position (background) and (b) with cell Z1 in comparison with a χ^2 minimum background line obtained from background measurements. These distributions are given for different time intervals, and the shape of the Poisson distributions is indicated by the dots. The background measurements are distributed around the χ^2 minimum line with an average difference zero, whereas the effect data dots show positive deviations from this line, most likely caused by *d-d* reactions in the sample. In this presentation, the shadow effect is still not taken into account, which explains the negative effect difference in the 1- to 220-h time interval.

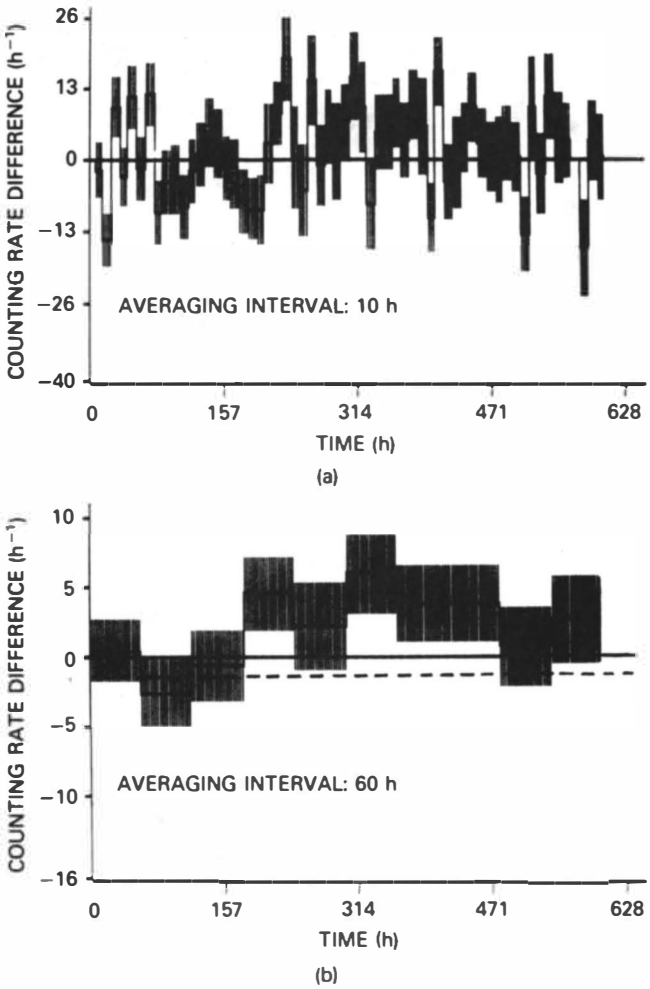

Fig. 3. Count rate differences averaged over (a) $\Delta t = 10$ h and (b) $\Delta t = 60$ h as a function of run time.

and valleys, a small but lengthy positive effect over several hundred hours was observed, arising only after 150 to 200 h of electrolysis.

These results are presented in another form in the averaging of count rate differences from zero up to a time t (the so-called integrated average count rate difference[5]), as presented in Fig. 4 for the three channel ranges. Whereas the integrated average for channel group 4 remains slightly negative, for channel groups 2 and 3, where *d-d* neutrons are expected, this value is definitely positive even compared to the uncorrected background level. If the properly corrected background levels (-2.0 ± 1.0), (-1.4 ± 1.0), and (-0.7 ± 0.7) h^{-1}, respectively, are used, the effect in channel groups 2 and 3 would become even more pronounced, whereas in channel group 4 the effect is almost zero within 1σ.

The cumulative count rate difference D_Σ in the three channel groups is presented in Fig. 5. It shows a pronounced positive effect for channel groups 2 and 3 and a negative effect in channel group 4. If the shadow effect is taken into account, the resulting zero line is declining, giving even more pronounced effects in channel groups 2 and 3, but it is nearly zero in channel group 4. A correct physical interpretation of the cumulative effect must take into account the sampling procedure of these measurements, which share the running time of the experimental cycle between three different cells, the empty position, and auxiliary measurements (such as checks of detector stability); thus, the real observation time of the cell with cathode Z1 is much less than the total duration of the cycle. Therefore, the total cumulative counting effect as shown in Fig. 5 has to be multiplied by a factor equal to the ratio between the integrated run time interval and the real observation duration within the time interval. For the integration interval shown in Fig. 5 (561 h with 99 effect measurements), this factor is 5.67. If the cumulative number of

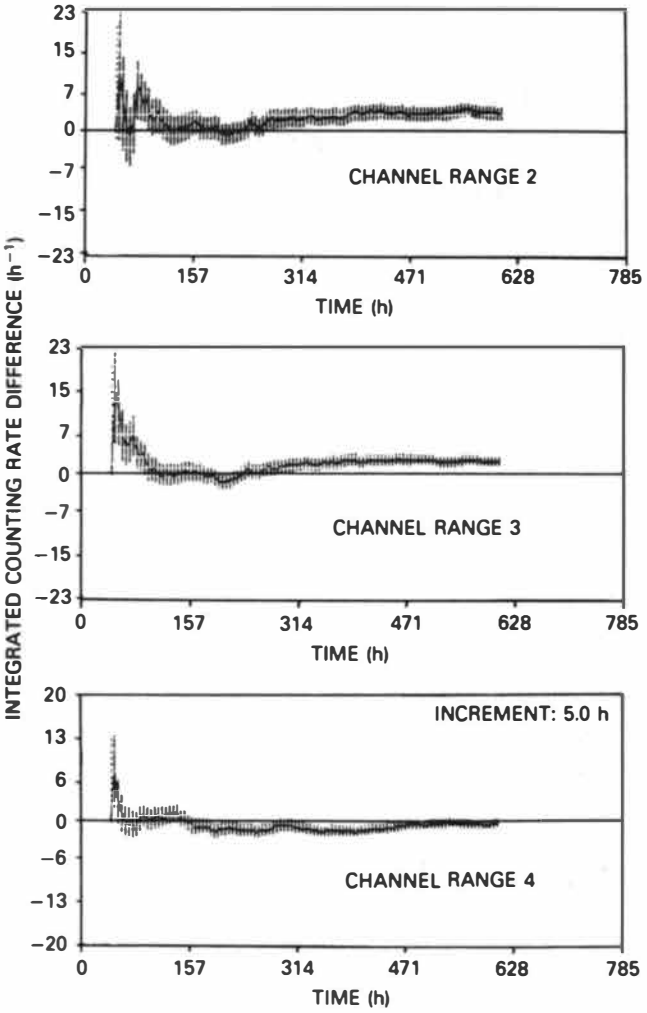

Fig. 4. Integrated count rate differences for channel ranges 2, 3, and 4 as a function of run time; the dotted lines are the effective (corrected) background level.

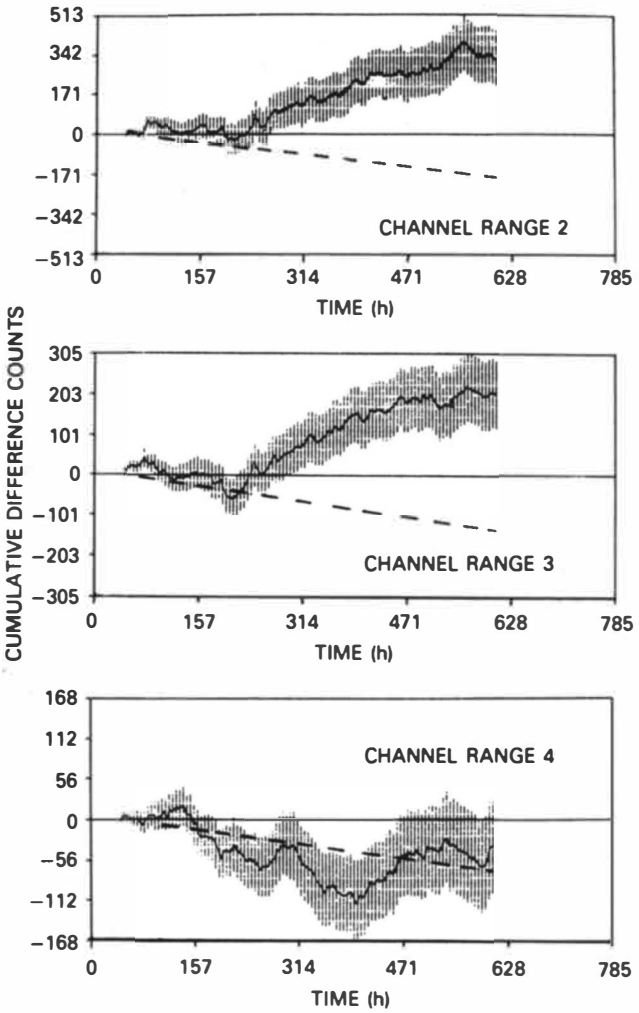

Fig. 5. Cumulative count rate differences for channel ranges 2, 3, and 4 as a function of run time; the dotted line shows the effective background level due to the shadow effect.[5]

fission events has to be determined, the count rate must also be multiplied by a factor of 20 because of the 5% neutron detection efficiency for channel group 2 (for channel group 3, the efficiency is 3%, which corresponds to a multiplication factor of 33.3). The 5% neutron detection efficiency includes the 20% efficiency of the detector for *d-d* neutrons in channel range 2 and a geometrical factor of 0.25 (see Ref. 5). Near the end of the integration interval, the numbers of effect counts with respect to the effective background lines are estimated to be 535 ± 80 and 345 ± 65 for channel ranges 2 and 3, respectively. Therefore, the cumulative number of counts in channel groups 2 and 3 corresponds, on the average, to ~(6.26 ± 1.1) × 10^4 reaction events within 561 h.

Finally, in Fig. 6, the proton-recoil spectra per hour for cell Z1 and the empty position, as well as their difference (histogram), are shown as a result of averaging within the 200- to 500-h time interval and for 0.1-MeV PRE intervals. The shadow effect is not taken into account in this figure. If it were, the effective background line would be below the zero line again and would decline from the right to the left because of the shape of the background neutron spectrum. Even without this correction, the observed proton-recoil spectrum is in accordance with the expectation that *d-d* neutrons are detected in this experiment.

DISCUSSION

The plasma model described by Seeliger and Meister[5] provides some explanation for the time structure of effects observed experimentally. From the average count rate differences presented in Fig. 3, the average *d-d* reaction rate $\dot{N}^{d\text{-}d}$ can be obtained, taking into account the detection efficiency for *d-d* neutrons. Following the model, the time structure of the average reaction rate is given by

$$\dot{N}^{d\text{-}d} = (n_D^{max})^2 \frac{\pi d^2 l}{4} - \left[1 - \exp\left(-\frac{t}{t_L}\right)\right]^2 \exp\left(-\frac{t}{t_L}\right) \kappa \lambda_{d\text{-}d}^{Pl} \sim \left[1 - \exp\left(-\frac{t}{t_L}\right)\right]^2 \exp\left(-\frac{t}{t_L}\right) , \quad (1)$$

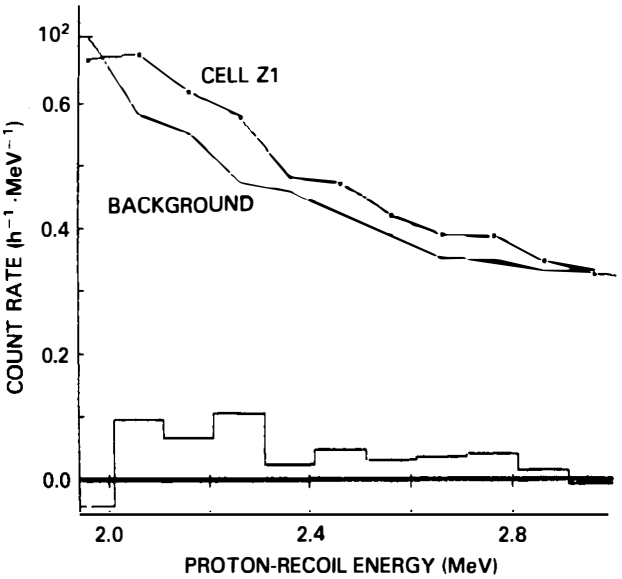

Fig. 6. Proton-recoil spectra for cell Z1 and background measurements averaged over time interval $\Delta t = 200$ to 500 h (upper part) and the corresponding difference spectrum in 0.1-MeV energy bins (lower part).

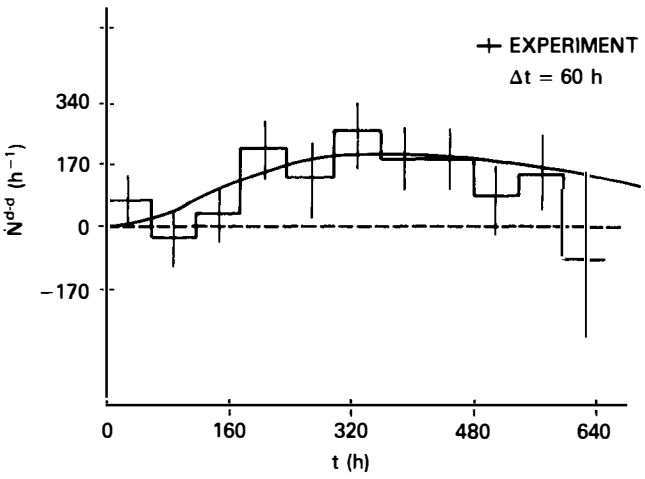

Fig. 7. Reaction rates for Z1 averaged over 60-h intervals in channel range 3; the histogram indicates data from the experiment; the solid curve is generated by calculation using Eq. (1); the dotted line indicates the effective background level.

where

$$t_L = \frac{dn_D^{max}}{4S_0} = \text{loading time constant} \quad (2)$$

$$\kappa = \exp\left(-\frac{V_0}{kT}\right) = \text{fraction of mobile particles} \quad (3)$$

$\lambda_{d\text{-}d}^{Pl} = d\text{-}d$ fusion rate per second.[6]

For practical calculations, the following parameters are used (for a more detailed explanation and justification, see Ref. 6):

$n_D^{max} = 6.8 \times 10^{22}$ (cm^{-3}) = maximum achievable deuteron density corresponding to $PdD_{1.0}$ (which, however, is not achieved in this experiment)

$S_0 = 3.12 \times 10^{16}$($cm^{-2} \cdot s^{-1}$) = initial particle flow into the metal (this corresponds to an electric current of 5 $mA \cdot cm^{-2}$)

$V_0 = 0.2$ eV = activation energy for diffusion of deuterium in palladium

$T = 320$ K = temperature of electrolyte, typical for this experiment (because of the cell cooling in an external water basin[5])

$k = 8.617 \times 10^{-5}$ ($eV \cdot K^{-1}$) = Boltzmann constant.

The loading time constant determines the gross structure of the experimental effects observed, and under the assumptions mentioned above, it amounts to $t_L \simeq 350$ h.

In Fig. 7, the $d\text{-}d$ reaction rate obtained from experimental count rate differences averaged over 60-h time intervals for channel group 3 is shown. In this figure, the shape of the model curve from Eq. (1) is also plotted. From the comparison between the absolute value of $\dot{N}^{d\text{-}d} = (180 \pm 30)\ h^{-1}$ in the area of its maximum (near $t \simeq t_L$) and Eq. (1), the $d\text{-}d$ fusion rate of

$$\lambda'_{d\text{-}d} = (1.30 \pm 0.22) \times 10^{-44}\ (s^{-1}) \quad (4)$$

is obtained.

The integrated average reaction rate $\langle \dot{N}^{d\text{-}d} \rangle$ from this model[6] is predicted to be

$$\langle \dot{N}^{d\text{-}d} \rangle \equiv \frac{1}{t}\int_0^t \dot{N}^{d\text{-}d}\,dt$$

$$= \frac{\pi}{4}(n_D^{max})^2 d^2 l \frac{t_L}{t} \times \left\{\frac{1}{3} - \exp\left(-\frac{t}{t_L}\right) \times \left[1 - \exp\left(-\frac{t}{t_L}\right) + \frac{1}{3}\exp\left(-\frac{2t}{t_L}\right)\right]\right\} \cdot \kappa\lambda_{d\text{-}d}$$

$$\sim \frac{1}{x}\left\{\frac{1}{3} - \exp(-x) \times \left[1 - \exp(-x) + \frac{1}{3}\exp(-2x)\right]\right\}, \quad (5)$$

with $x = t/t_L$.

In Fig. 8 the shape of this curve is compared with the average integrated reaction rate obtained from experimental count rate differences for channel group 3. Again, it is evident that the gross structure of long-term behavior is reasonably described by the model prediction. From comparison between the absolute value $\langle \dot{N}^{d\text{-}d} \rangle = (110 \pm 20)\ h^{-1}$ near the end of the experimental cycle, at $t \simeq 1.71 t_L$, the $d\text{-}d$ fusion rate can be obtained again, resulting in

$$\lambda''_{d\text{-}d} = (1.08 \pm 0.19) \times 10^{-44}\ (s^{-1}) .$$

Within the estimated uncertainties, both values for $\lambda_{d\text{-}d}^{Pl}$ agree with each other, although they are obtained from overlapping but not identical experimental data. (The term $\lambda'_{d\text{-}d}$ is determined mainly by data points up to $t = 400$ h, while $\lambda''_{d\text{-}d}$ is derived from all data points up to the end of the cycle.)

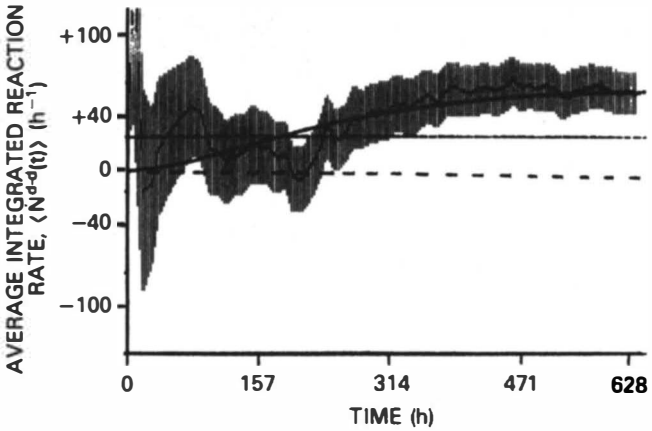

Fig. 8. Average integrated reaction rate $\langle \dot{N}^{d\text{-}d} \rangle$ for Z1 and channel range 3 as a function of running time. Experimental data are compared with the model calculation following Eq. (5) (solid curve). The dotted line indicates the effective background level.

The average *d-d* fusion rate obtained from both methods is

$$\lambda_{d\text{-}d}^{Pl} = (1.19 \pm 0.15) \times 10^{-44}\ (s^{-1}) \ .$$

CONCLUSION

The experiment used a compact palladium cylinder for >600 h and a sensitive fast neutron spectrometer. It showed very weak but definite signals of neutrons that most likely result from *d-d* reactions. However, this effect became observable experimentally only after >200 h of loading because of the large loading time constant of such a massive electrode. After this, strongly fluctuating positive effects occurred during several hundred hours with slowly decreasing intensity.

The average long-term behavior of the effects observed was comparable with the predictions of a crude plasmalike model. The fluctuating character of the effects seems to indicate, however, that the particle flow inside the metal was not a continuous, smooth one as assumed in this model, but rather it behaved as statistically distributed microavalanches transporting the deuterons into the depth of the metal.

The cumulative number of reaction events that occurred during the measuring cycle was of the order of $(6.26 \pm 1.1) \times 10^4$.

The plasma fusion rate $\lambda_{d\text{-}d}^{Pl}$ as determined from the experiment has to be compared directly with calculations of the so-called reactivity $\langle v_d \sigma_{d\text{-}d} \rangle$ in a plasma (see, for instance, papers by Scalia[7] and Rice et al.[8]). However, besides the usual averaging over the Maxwellian velocity distribution, the electron screening and dynamic enhancement of the tunneling probability should also be taken into account to get a comparable order of magnitude for $\lambda_{d\text{-}d}^{Pl}$ from theory and experiment. Further work on this is in progress, both in the direction of testing other samples experimentally as well as in the development of elaborate physical descriptions.

REFERENCES

1. S. E. JONES et al., "Observation of Cold Nuclear Fusion in Condensed Matter," *Nature*, **338**, 737 (1989).

2. H. O. MENLOVE et al., "Measurement of Neutron Emission from Ti and Pd in Pressurized D_2 Gas and D_2O Electrolysis Cells," LAUR:89-1974, Los Alamos National Laboratory (July 27, 1989).

3. D. SEELIGER et al., "Search for DD-Fusion Neutrons During Heavy Water Electrolysis," *Electrochim. Acta*, **34**, 991 (1989).

4. D. SEELIGER, "Physikalische Probleme der Untersuchung zur Kernfusion in kondensierter Materie," *Isotopenpraxis*, **26**, 384 (1990).

5. M. BITTNER et al., "Method for Investigation of Fusion Reactions in Condensed Matter," *Fusion Technol.*, **18**, 120 (1990).

6. D. SEELIGER and A. MEISTER, "A Simple Plasma Model for the Description of *d-d* Fusion in Condensed Matter," *Fusion Technol.*, **19**, 2114 (1991).

7. A. SCALIA, "The Nuclear Fusion Rate for Reactions $^2H(d,n)$, $^2H(d,p)$," *Nuovo Cimento*, **101A**, 795 (1989); see also *Nuovo Cimento*, **102A**, 953 (1989).

8. R. A. RICE et al., "The Role of Velocity Distribution in Cold Deuterium-Deuterium Fusion," *Fusion Technol.*, **18**, 147 (1990).